

Better age estimation using UV-optical colours: breaking the age-metallicity degeneracy

S. Kaviraj^{1*}, S. -C. Rey^{2,3,4}, R. M. Rich⁵, S. -J. Yoon³ and S. K. Yi³

¹ *Department of Physics, University of Oxford, Keble Road, Oxford OX1 3RH, UK*

² *Department of Astronomy and Space Science, Chungnam National University, Daejeon 305-764, Korea*

³ *Yonsei University, Center for Space Astrophysics, Seoul 120749, Korea*

⁴ *California Institute of Technology, 1200 E. California Blvd. Pasadena, CA 91125, USA*

⁵ *Department of Physics and Astronomy, UCLA, 430 Portola Plaza, Box 951547, Los Angeles, CA 90095-1547*

19 November 2006

ABSTRACT

We demonstrate that the combination of GALEX *UV* photometry in the *FUV* (~ 1530 angstroms) and *NUV* (~ 2310 angstroms) passbands with optical photometry in the standard *U, B, V, R, I* filters can efficiently break the age-metallicity degeneracy. We estimate well-constrained ages, metallicities and their associated errors for 42 GCs in M31, and show that the full set of *FUV, NUV, U, B, V, R, I* photometry produces age estimates that are ~ 90 percent more constrained and metallicity estimates that are ~ 60 percent more constrained than those produced by using optical filters alone. The quality of the age constraints is comparable or marginally better than those achieved using a large number of spectroscopic indices.

Key words: galaxies: elliptical and lenticular, cD – galaxies: evolution – galaxies: formation – galaxies: fundamental parameters

1 INTRODUCTION

Broad-band photometry has traditionally played a key role in the study of a variety of astrophysical objects. Often, it is of interest to decipher the formation histories of various systems, e.g. globular clusters (GCs), by age-dating them. The vast majority of studies have so far been restricted to *optical* photometry e.g. (Yi et al. 2004; Peng et al. 2004). However, the use of optical photometry has been plagued by the well-known *age-metallicity degeneracy* (AMD) whereby young, metal-rich stellar populations produce optical colours which are indistinguishable from those due to old metal-poor populations (Worthey 1994). It is therefore difficult to simultaneously pin down the age and metallicity of an object using optical colours alone. While combinations of metallicity-sensitive and age-sensitive colours, e.g. $U - B$ versus $B - V$ (Yi et al. 2004), can produce rough estimates of age and metallicity, the errors on these estimates can be extremely large. For example, the age uncertainty could be as large as the age of the universe (e.g. Yi et al. 2004)!

Ages can be better studied, and the AMD alleviated spectroscopically, by combining a sufficient number of age and metallicity-sensitive line indices (see e.g. Trager et al. 2000; Proctor & Sansom 2002; Caldwell et al. 2003). For example, Trager et al. (2000) use the H_{β} , Mg *b* and $\langle \text{Fe} \rangle$ line

strengths to estimate well-constrained SSP-equivalent ages and metallicities for a sample of local elliptical galaxies. Similarly, Proctor & Sansom (2002) use a combination of 24 line indices to break the AMD and produce SSP-equivalent parameters with small uncertainties for the central regions of 32 systems taken from both the Virgo cluster and the field. However, such methods rely on accurate measurements of a sufficiently large ensemble of indices for each object of interest.

Rest-frame *UV* flux, shortward of ~ 3000 angstroms, provides an attractive alternative. From a theoretical point of view, it has already been suggested (e.g. Yi 2003) that the *UV* spectral ranges may provide a better handle on the ages of objects and thus reduce the AMD. It is the aim of this Letter to *quantify* the usefulness of the *UV* in breaking the AMD and providing robust age estimation, especially in the context of simple populations like GCs. If the addition of *UV* photometry were to provide comparable constraints in the age-metallicity parameter space as, for example, large numbers of spectral line indices, then the advent of large-scale *UV* photometry from the GALEX mission (Martin et al. 2005) could provide an accessible means of age-dating a wide variety of nearby objects using photometry alone. For example, in its Medium Imaging Survey (MIS) mode, which reaches a depth of 22.6 and 22.7 AB in *FUV* and *NUV* respectively, GALEX detects more than 90 percent of bright ($r < 16.8$), nearby ($0 < z < 0.11$) early-type galaxies ob-

* E-mail: skaviraj@astro.ox.ac.uk

served by the SDSS (see Figure 1 in Kaviraj et al. 2006). Given the large-scale nature of the GALEX dataset and the excellent overlap with existing optical surveys, it is therefore possible to incorporate *UV* photometry into age-dating analyses of stellar populations.

In this study we combine GALEX broad-band *UV* photometry in two passbands (*NUV*: ~ 2310 angstroms and *FUV*: ~ 1530 angstroms) with optical photometry in the standard *U, B, V, R, I* filters to simultaneously estimate the ages and metallicities of GCs in M31. The GCs are drawn from the catalogue of Rey et al. (2005) who have combined GALEX imaging of the M31 system with the optical catalogue of Barmby et al. (2000). The use of GCs is motivated by the fact that their star formation histories (SFHs) can be adequately parametrised by simple stellar populations (SSPs) of a given age and metallicity alone. They are therefore ideal test objects to demonstrate the usefulness of *UV* photometry in constraining the age-metallicity parameter space. Although we derive both age and metallicity, our emphasis is on the quality of the *age estimation*, as this is of primary importance in the determination of formation histories. Note that, while the stellar models used here (described below) assume solar abundance ratios, GC age estimates derived using *optical* colours tend to be lower by ~ 8 percent if alpha-enhanced ($[\alpha/Fe] = 0.3$) ratios are considered (Kim et al. 2002).

In the following sections, we compare the quality of the constraints on age and metallicity with and without *UV* photometry, investigate how the constraints change as various filters are excluded from the parameter estimation and compare our purely photometric analysis to previous studies that have used spectroscopic indicators to estimate SSP-equivalent ages and metallicities for a variety of systems.

2 PARAMETER ESTIMATION

We begin by outlining the method used for parameter estimation. For a vector \mathbf{X} denoting parameters in the model and a vector D denoting the measured observables (data),

$$\text{prob}(\mathbf{X}|D) \propto \text{prob}(D|\mathbf{X}) \times \text{prob}(\mathbf{X}), \quad (1)$$

where $\text{prob}(\mathbf{X}|D)$ is the probability of the model given the data (which is the object of interest), $\text{prob}(D|\mathbf{X})$ is the probability of the data given the model and $\text{prob}(\mathbf{X})$ is the prior probability distribution of the model parameters. Assuming a uniform prior in our model parameters and gaussian errors gives

$$\text{prob}(D|\mathbf{X}) \propto \exp(-\chi^2/2), \quad (2)$$

where $\exp(-\chi^2/2)$ is the likelihood function and χ^2 is defined in the standard way. $\text{prob}(\mathbf{X}|D)$ is a *joint* PDF, dependent on all the model parameters. To isolate the effect of a single parameter X_1 in, for example, a two parameter model ($\text{prob}(\mathbf{X}|D) \equiv \text{prob}(X_1, X_2|D)$) we can integrate out the effect of X_2 to obtain the *marginalised* PDF for X_1 :

$$\text{prob}(X_1|D) = \int_0^\infty \text{prob}(X_1, X_2|D) dX_2. \quad (3)$$

In our analysis, the parameters \mathbf{X} in the model are

the age (t) and metallicity (Z) of the SSP in question, and the observables are colours constructed from *FUV, NUV, U, B, V, R, I* photometry. We choose a uniform prior in t , in the range 0 to 14 Gyrs. We set the maximum allowed age to 14 Gyrs using the WMAP estimate for the age of the universe (13.7 Gyrs, Spergel et al. 2003) - we note that structure formation probably commences ~ 0.2 - 0.5 Gyrs after the creation of the Universe. For the metallicity Z , we use a uniform prior in the range -2.3 to 0.36 dex, which are essentially the metallicity limits of the stellar models. For each GC analysed, we marginalise the age and metallicity parameters, take the *peak* (x_0) of the marginal PDF $P(x)$ as the best estimate and *define* one-sigma limits x_+ and x_- as $\int_{x_0}^{x_+} P(x) dx = 0.34 \int_{x_0}^\infty P(x) dx$ and $\int_{x_-}^{x_0} P(x) dx = 0.34 \int_{-\infty}^{x_0} P(x) dx$ respectively.

The *uncertainty* in the parameter is then $(x_+ - x_-)$. Note that we do not consider correlated errors in the two quantities.

3 AGE AND METALLICITY CONSTRAINTS

Young stellar populations (< 1 Gyr old) emit a substantial proportion of their flux in the ultraviolet, making *UV* photometry a good indicator of their presence. However, *UV* flux can also be generated by old, evolved stages of stellar evolution. Due to their longevity, hot, core Helium-burning horizontal-branch (HB) stars and their progeny are thought to be the dominant *UV* sources in old stellar populations, such as GCs and elliptical galaxies. While metallicity is the dominant parameter controlling the HB morphology of Galactic halo-like stellar populations, the second parameter governing the properties of the HB has been the subject of much debate (e.g. Sarajedini et al. 1997; Bellazzini et al. 2001), consensus favouring age differences between clusters as the major second parameter affecting HB morphology (e.g. Lee 1994).

The stellar models used in this study employ detailed prescriptions for the systematic variation of HB morphology with metallicity and age, and are well-calibrated to Galactic GC populations and the integrated *UV*-optical photometry of local elliptical galaxies (see Yi 2003, and references therein). Main-sequence to Red Giant Branch isochrones employed in these models are described in Yi et al. (2001) and the HB stellar tracks are described in Yi et al. (1997). The flux library employed is from Lejeune et al. (1998).

In Figure 1 we illustrate the onset of *UV* flux in the models with the appearance of horizontal branch stars, as the stellar population evolves through intermediate ages of 4 and 7 Gyrs to an age comparable to stars in the Galactic halo (~ 13 Gyrs). The age estimation procedure essentially fits the observed shape of the *UV*-optical continuum to the models. In this context we note that, although the shape of the *UV* spectrum from a young and old population can appear similar, the slope of their optical continua are very different, which allows them to be differentiated easily. Thus, with access to a reasonably large set of *UV* and optical filters, age determinations of stellar populations such as GCs can be performed with reasonably good accuracy, as we demonstrate below.

The purpose of this Letter is not to perform a rigorous study of the entire M31 GC system but to demonstrate

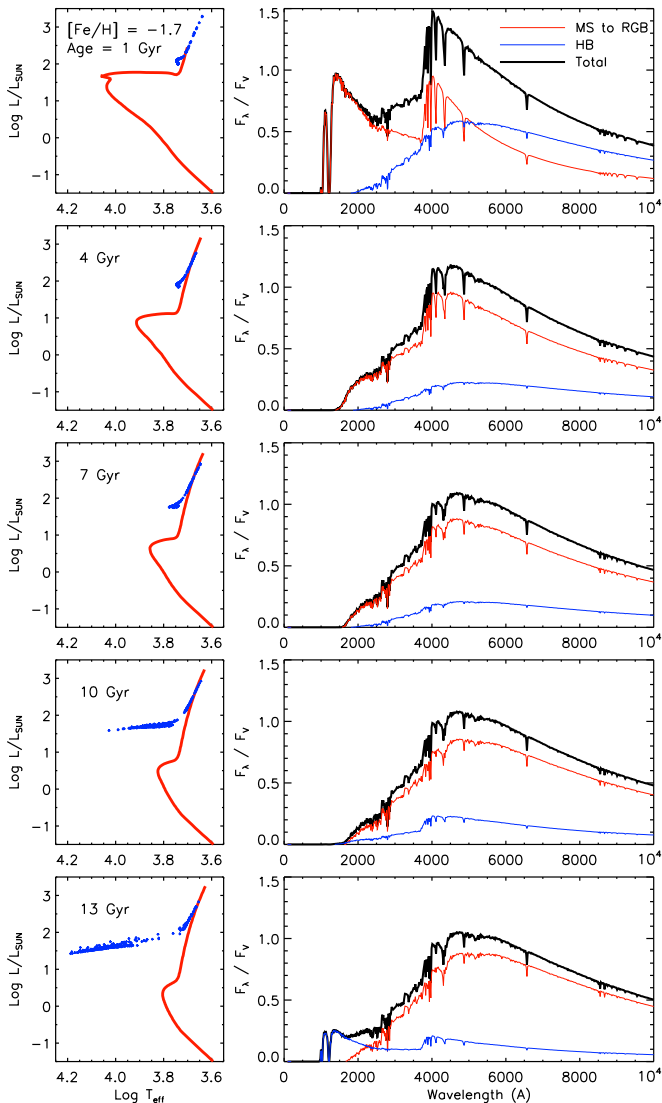


Figure 1. *UV* flux from old populations due to the onset of the horizontal branch population (top to bottom). Intermediate age populations (~ 4 -7 Gyrs old) output negligible amounts of *UV* flux. The contributions from the MS-RGB and HB phases are shown in red and blue respectively. In all panels $[\text{Fe}/\text{H}] = -1.7$ dex. The HB develops at higher (lower) ages for $[\text{Fe}/\text{H}]$ greater (lower) than -1.7 dex. For example, for $[\text{Fe}/\text{H}] \sim -1.2$ and $[\text{Fe}/\text{H}] \sim -2.1$ dex, the HB develops at 12 and 8 Gyrs respectively. Note that this implies that metal-rich GCs will have weaker age constraints due to the later rise of the HB.

the usefulness of *UV* photometry in reducing the AMD and present a method that exploits this property. We therefore extract parts of Rey et al. (2005)’s catalogue that best satisfy this aim - GCs with good detections in GALEX, which have the full set of optical *U*, *B*, *V*, *R*, *I* photometry and lie in regions of relatively low Galactic reddening ($E_{B-V} < 0.2$). We find 42 objects matching this description in the catalogue.

We begin by investigating the age and metallicity constraints achieved using seven broad-band colours: $FUV - V$, $NUV - V$, $FUV - NUV$, $U - B$, $B - V$, $V - R$, $V - I$ (Figure 2) and compare them to the scenario where the *UV* colours are absent (Figure 3). The large AMD due to using only opti-

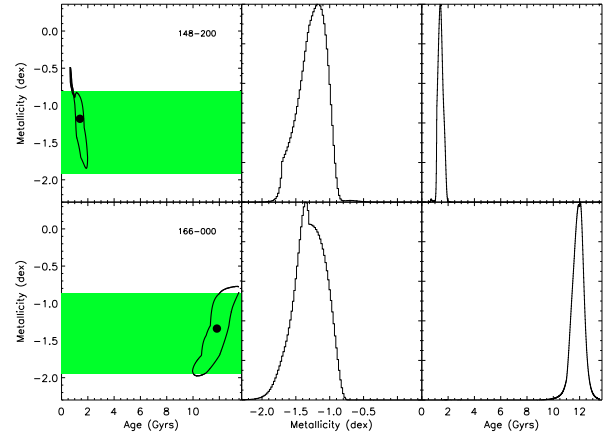


Figure 2. Age and metallicity constraints from *UV* and optical photometry for two GCs in our sample. LEFT COLUMN: Best-fit position and one-sigma contour. MIDDLE COLUMN: Marginalised metallicity PDF (normalised). RIGHT COLUMN: Marginalised age PDF (normalised). Top row shows a young cluster (148-200) and bottom row shows an old cluster (166-000). The green region shows a spectroscopic metallicity measurement taken from Barmby et al. (2000) or Perrett et al. (2003).

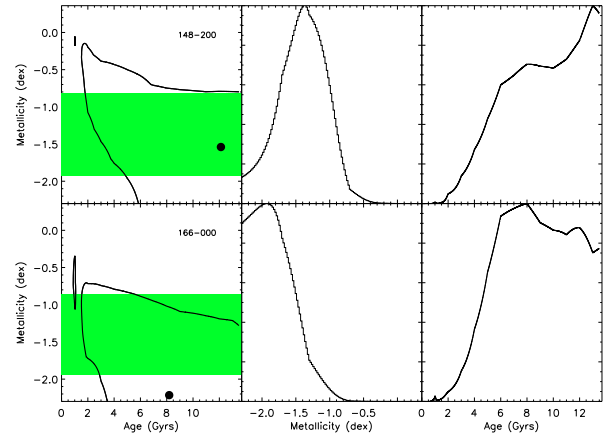


Figure 3. Same as Figure 2 but using optical photometry only.

cal passbands is clearly visible in Figure 3. The effect on the age estimation is severe - since the parameter space inside the contour is indistinguishable in terms of the goodness of fit (the *best-fit* value has very limited significance), the age of either GC can be anywhere between 2 and 13 Gyrs. The age constraint is far superior when *UV* photometry is added. The young cluster (148-200) now has a well-constrained age of 0.5-2 Gyrs and the old cluster has an age of 10-13 Gyrs. The photometry suggests that both clusters are metal-poor ($[\text{Fe}/\text{H}] < -0.5$), in agreement with the spectroscopically determined metallicity (green region).

In Figure 4 we summarise the age and metallicity constraints from the full set of *UV* and optical photometry for the 42 GCs in our sample. The age constraints are robust, with the full extent of the age uncertainties lying between

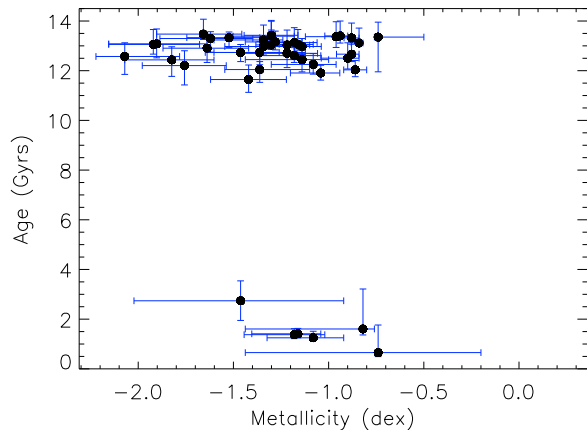


Figure 4. Age and metallicity constraints from the full set of *UV* and optical photometry from our 42 GCs.

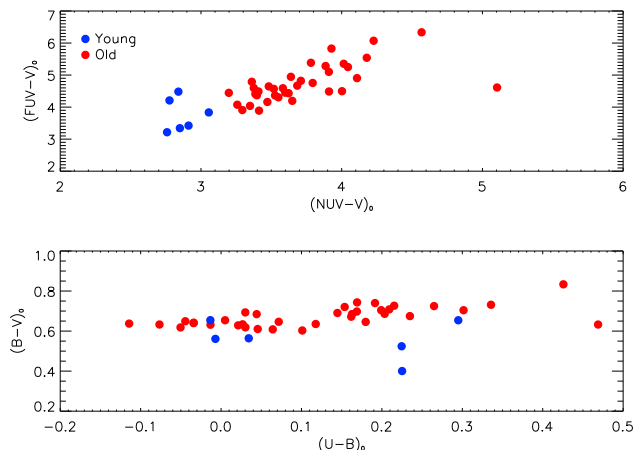


Figure 5. TOP PANEL: Comparison of the best-fit ages of GCs to their $(NUV - V)_0$ and $(FUV - V)_0$ colours. BOTTOM PANEL: Comparison of the best-fit ages of GCs to their $(U - B)$ and $(B - V)$ colours.

0.1 and 3 Gyrs. The metallicity constraint is not as robust as the age uncertainties, which is expected since the *UV* is a better indicator of age than metallicity. We find that, although the photometric metallicity constraint overlaps with its spectroscopic equivalent in all cases, the spectroscopic constraint is invariably more robust.

In Figure 5 we compare the best-fit ages of each GC to their photometric colours. Contrary to the optical scenario, we can use the best-fit ages in this case *because the age uncertainties are small*. We find that GCs with well-constrained young ages tend to be bluer in both the $(NUV - V)_0$ and $(FUV - V)_0$ colours. In contrast, the comparison to optical colours is more ambiguous - while there is an indication that the young GCs are bluer in $(B - V)_0$, there is no clear separation between the young and old populations, as a result of the AMD.

In practice, a full set of *FUV*, *NUV*, *U*, *B*, *V*, *R*, *I* pho-

tometry may not always be available. For example, good quality photometry is far more difficult to achieve in the *U* band than in longer optical wavelengths. It is therefore instructive to compare the quality of the age and metallicity constraints when a subset of these passbands is excluded from the parameter estimation. We quantify this comparison in Table 1. Since using only optical filters always gives the largest uncertainties, we compute the ratio of the uncertainty from using a particular set of filters to the uncertainty when only optical filters are used. We show the average values of these ratios, for the age constraints (f_t - column 9) and for the metallicity constraints (f_Z - column 10). A smaller value thus indicates a *better* constraint and smaller uncertainty in the estimation of age or metallicity. The filter sets are listed in order of the quality of the *age constraint* i.e. the first row indicates the filter set with the *best* age constraint. The constraints are virtually identical as long as either the *R* or *I* filters are present - we have therefore put them in the same column in Table 1.

Looking first at constraints on the age estimates, we find that, for the full set of *FUV*, *NUV*, *U*, *B*, *V*, *R*, *I* filters (row 1), the size of the marginalised age errors are ~ 10 percent of the optical-only case ($f_t = 0.12$) i.e. the age estimates are ~ 90 percent better constrained than those from using optical filters alone (row 7). Removing the longer wavelength *R*, *I* bands (row 2) or the shorter wavelength *U* band (row 3) slightly weakens the age constraint compared to the full set of filters. If only one *UV* filter is available, it is preferable to combine the *FUV* passband with optical photometry (row 5) than the *NUV* passband (row 6).

Similarly, the comparison of metallicity estimates (values of f_Z in Table 1) indicates that adding *UV* photometry to the optical *U*, *B*, *V*, *R*, *I* filters (or a subset of them) improves the metallicity estimates by approximately ~ 60 percent compared to the optical-only case. f_Z refers to the underlying metallicity Z , converted from the $[\text{Fe}/\text{H}]$ value using Table 2 of Yi et al. (2001).

4 COMPARISON WITH SPECTROSCOPIC METHODS

We now compare the quality of our photometric age and metallicity constraints with three studies which derive these parameters using spectroscopic line indices. The Trager et al. (2000) study uses the H_β , $\text{Mg } b$, $\text{Fe}5270$ and $\text{Fe}5335$ indices to obtain tightly-constrained SSP ages for a sample of local elliptical galaxies, with age uncertainties of $\sim 0.5 - 1.5$ Gyrs for young objects and $\sim 2 - 3$ Gyrs for old and intermediate age objects (see their Table 6A). In a similar work, Proctor & Sansom (2002) combine line strength measurements of 24 age and metallicity sensitive indices for the central regions of 32 galaxies in both the Virgo cluster and the field. Their age uncertainties are in the range $\sim 1 - 3$ Gyrs (see their Table 10 or Figure 12). In a more recent work, Beasley et al. (2004) measure 24 indices in the Lick system (Worthey & Ottaviani 1997; Trager et al. 1998) for a sample of 30 globular clusters in M31. The uncertainties in their age-estimates are $\sim 0.2-1.25$ Gyrs (see their Figure 12). Looking at Figure 4 we see that the uncertainties in our photometric age-determinations are $\sim 0.1 - 2$ Gyrs for the young clusters and $\sim 0.5 - 3$ Gyrs for the old clusters.

Table 1. Comparison of the quality of age and metallicity constraints for different filter sets. f_t (f_z) is the ratio of the age (metallicity) uncertainty using the filters in a given row to the age uncertainty using optical filters only (row 7). The filter sets are listed in order of the quality of the *age constraint* i.e. the first row indicates the filter set with the *best* age constraint.

	<i>FUV</i>	<i>NUV</i>	<i>U</i>	<i>B</i>	<i>V</i>	<i>R,I</i>	f_t	f_z
1	✓	✓	✓	✓	✓	✓	0.12	0.31
2	✓	✓	✓	✓	✓	×	0.23	0.37
3	✓	✓	×	✓	✓	✓	0.26	0.38
4	✓	✓	×	✓	✓	×	0.26	0.39
5	✓	×	✓	✓	✓	✓	0.39	0.47
6	×	✓	✓	✓	✓	✓	0.47	0.51
7	×	×	✓	✓	✓	✓	1.00	1.00

We therefore find that our photometric analysis produces comparable age constraints to the spectroscopic studies.

However, our metallicity constraints are arguably worse than those in the spectroscopic studies mentioned above. While we do not resolve the metallicity to better than ± 0.3 to 0.5 dex for any cluster, spectroscopic constraints on metallicity are generally tighter, of the order of ~ 0.1 dex. This is expected, not only since the *UV* passbands are better indicators of age than of metallicity but because the combination of multiple metallicity-sensitive indices in these studies results in better metallicity constraints than can be achieved with photometry alone.

5 CONCLUSIONS

In this study we have demonstrated that the combination of *FUV* (~ 1530 angstroms) and *NUV* (~ 2310 angstroms) photometry with optical observations in the standard *U, B, V, R, I* filters can efficiently break the AMD caused by using optical filters alone. We have estimated ages, metallicities and their associated uncertainties for a sample of 42 GCs in M31 for which we have the full set of *UV* and optical photometry. We have found that using the full set of *FUV, NUV, U, B, V, R, I* filters produces age estimates that are ~ 90 percent more constrained and metallicity estimates that are ~ 60 percent more constrained than those produced by using optical filters alone. The quality of the age constraints is comparable to those achieved using a large number of spectroscopic line strength indices. We find that if only one *UV* passband is available, then combining the *FUV* rather than the *NUV* with optical photometry is preferable in terms of constraining ages. Finally, while there is overlap between our photometrically determined metallicity ranges and the corresponding constraints from spectroscopic studies for GCs in our sample, the photometric metallicity constraints are generally weaker than their spectroscopic counterparts.

We note that, since the *UV* is produced by either young (< 2 Gyr old) or evolved (> 10 Gyr old) stars, it is insensitive to intermediate-age populations, leading to a lack of intermediate-age GCs in Figure 4. To conclude, we suggest that broad-band *UV* photometry from the GALEX mission (which, at completion, will survey the entire local universe) could be used as an effective age indicator to break the AMD, and as a useful proxy for spectroscopic methods in constraining the age-metallicity parameter space.

6 ACKNOWLEDGEMENTS

We thank Andrés Jordán, Roger Davies, Rachel Somerville and Claudia Maraston for many useful discussions. We are grateful to the referee, Anne Sansom, for an insightful review that greatly improved the quality of the manuscript. SK acknowledges a PPARC DPhil scholarship, a Leverhulme Early-Career Fellowship and Research Fellowships from Worcester College, Oxford and the BIPAC institute at Oxford. SCR acknowledges support through the Korea Research Foundation Grant, funded by the Korean Government (MOEHRD) (KRF-2005-202-C00158). SJY and SKY acknowledge support through Grant No. R01-2006-000-10716-0 from the Basic Research Program of the Korea Science & Engineering Foundation.

REFERENCES

- Barmby P., Huchra J. P., Brodie J. P., Forbes D. A., Schroder L. L., Grillmair C. J., 2000, *AJ*, 119, 727
 Beasley M. A., Brodie J. P., Strader J., Forbes D. A., Proctor R. N., Barmby P., Huchra J. P., 2004, *AJ*, 128
 Bellazzini M., Pecci F. F., Ferraro F. R., Galleti S., Catelan M., Landsman W. B., 2001, *AJ*, 122, 2569
 Caldwell N., Rose J. A., Concannon K. D., 2003, *AJ*, 125, 2891
 Kaviraj S., GALEX Science Team 2006, *ApJ* - GALEX dedicated issue (Dec 2007), astro-ph/0601029
 Kim Y.-C., Demarque P., Yi S. K., Alexander D. R., 2002, *ApJS*, 143, 499
 Lee Y.-W., 1994, *ApJ*, 430, L113
 Lejeune T., Cuisinier F., Buser R., 1998, *A&AS*, 130, 65
 Martin D. C., GALEX collaboration 2005, *ApJ*, 619, L1
 Peng E. W., Ford H. C., Freeman K. C., 2004, *ApJ*, 602, 705
 Perrett K. M., Stiff D. A., Hanes D. A., Bridges T. J., 2003, *ApJ*, 589, 790
 Proctor R. N., Sansom A. E., 2002, *MNRAS*, 333, 517
 Rey S.-C., GALEX Science Team 2005, *ApJ*, 619, L119
 Sarajedini A., Chaboyer B., Demarque P., 1997, *PASP*, 109, 1321
 Spergel D. N., WMAP Team 2003, *ApJS*, 148, 175
 Trager S. C., Faber S. M., Worthey G., González J. J., 2000, *AJ*, 119, 1645
 Trager S. C., Worthey G., Faber S. M., Burstein D., González J. J., 1998, *ApJS*, 116, 1
 Worthey G., 1994, *ApJS*, 95, 107
 Worthey G., Ottaviani D. L., 1997, *ApJS*, 111, 377

- Yi S., Demarque P., Kim Y.-C., 1997, *ApJ*, 482, 677
Yi S., Demarque P., Kim Y.-C., Lee Y.-W., Ree C. H.,
Lejeune T., Barnes S., 2001, *ApJS*, 136, 417
Yi S. K., 2003, *ApJ*, 582, 202
Yi S. K., Peng E., Ford H., Kaviraj S., Yoon S.-J., 2004,
MNRAS, 349, 1493